International Journal of Pharmaceutics 420 (2011) 378–384

Contents lists available at SciVerse ScienceDirect

International Journal of Pharmaceutics

journal homepage: www.elsevier.com/locate/ijpharm

Pharmaceutical Nanotechnology

A 5-fluorouracil-loaded pH-responsive dendrimer nanocarrier for tumor targeting

Yiguang Jin[a,b,*], Xia Ren[a,b], Wei Wang[b], Lijing Ke[c,d], Erjuan Ning[a,b], Lina Du[a], Jeremy Bradshaw[c]

[a] Department of Pharmaceutical Sciences, Beijing Institute of Radiation Medicine, Beijing 100850, China
[b] Institute of Pharmacy, Pharmaceutical College of Henan University, Kaifeng 475004, China
[c] Royal (Dick) School of Veterinary Sciences, University of Edinburgh, Summerhall, Edinburgh EH9 1QH, Scotland, United Kingdom
[d] Institute of Biotechnology, Fuzhou University, 523 Gongye Road, Fuzhou 350002, China

ARTICLE INFO

Article history:
Received 16 May 2011
Received in revised form 9 August 2011
Accepted 31 August 2011
Available online 8 September 2011

Keywords:
5-Fluorouracil
Nanocarriers
pH-responsive
Poly(amidoamine)
Tumor targeting

ABSTRACT

A novel long-circulating and pH-responsive dendrimer nanocarrier was prepared for delivering 5-fluorouracil (5-FU) to tumors through the targeting of nanoparticles to the low pH environment of tumors. The nanocarrier, poly(2-(N,N-diethylamino)ethyl methacrylate) with methoxy-poly(ethylene glycol)-poly(amidoamine) (PPD), had a core–shell structure with 4.0 G poly(amidoamine) (PAMAM) as the core and parallel poly(2-(N,N-diethylamino)ethyl methacrylate) (PDEA) chains and methoxy-poly(ethylene glycol) (mPEG) chains as the shell. The PDEA chain was pH-responsive, and the PEG chains led to long circulation in blood vessels to achieve tumor targeting. The sizes, drug encapsulation and release of PPD nanocarriers showed high pH-dependency due to the PDEA chains, as they were hydrophilic at pH 6.5 and hydrophobic at pH 7.4. The encapsulation efficiency of 5-FU in PPD nanocarriers was as high as 92.5% through the pH transition. The release of 5-FU from PPD nanocarriers was much faster at pH 6.5 than at pH 7.4. The 5-FU-loaded nanocarrier had a long half-life after intravenous administration in mice and showed high tumor targeting. This nanocarrier composite also showed enhanced anticancer effects. PPD is a promising nanocarrier of anticancer drugs with high encapsulation, tumor targeting and pH-responsive release in tumors.

1. Introduction

Dendrimers are synthetic dendritic polymers with versatile, derivatizable, well-defined, compartmentalized chemical structures (Tomalia et al., 1985). Dendrimers function as nanomedicines against tumors, bacteria and viruses. They are also used as drug carriers to achieve organ targeting and/or controlled release *in vivo* based on nanoscale functionalized surface groups (Boas and Heegaard, 2004; Gillies and Fréchet, 2005; Svenson and Tomalia, 2005). Poly(amidoamine) (PAMAM) is one typical type of dendrimer with wide biomedical applications due to its low toxicity and highly functional surface groups (Esfand and Tomalia, 2001).

One major problem in cancer chemotherapy is the severe side effects of anticancer drugs due to their random distribution in the body. However, nanoscale particles readily penetrate tumor tissues based on their enhanced permeability and retention (EPR) effects (Amiji, 2007). Tumor-targeted drug delivery can be achieved using nanocarriers based on this EPR effect (Iyer et al., 2006). As such, a variety of nanoparticulate systems are used as carriers for anticancer agents (e.g., liposomes, nanoparticles, and polymeric micelles). However, naked nanoparticles would likely be taken up by the mononuclear phagocyte system due to opsonization after intravenous (i.v.) administration (Ishida et al., 2002).

Long-circulating particles that can escape phagocytosis have the opportunity to target tumors based on the EPR effect. Long poly(ethylene glycol) (PEG) chains can form a shell on the surface of particles to prevent opsonization (Moghimi et al., 2001). However, little drug loading and weak tumor targeting of nanocarriers hinder their current development (Cho et al., 2008).

PAMAM has a very small diameter (6.5 nm diameter for 6.0 G PAMAM) and is seemingly suitable for anticancer drug delivery. However, the inner space of PAMAM is open, so entrapped drugs tend to diffuse into the surroundings if there is no strong interaction between the drugs and the interior of the dendrimers. For example, methotrexate and doxorubicin were readily released from drug-loaded poly(ethylene glycol)$_{2000}$-attached 4.0 G PAMAM dendrimers in isotonic solutions (Kojima et al., 2000). The drug loaded in dendrimer carriers is then ready for release into the circulation after i.v. administration, but not is selectively released into tumor tissues. Furthermore, covalently coupled methotrexate in

* Corresponding author at: Department of Pharmaceutical Sciences, Beijing Institute of Radiation Medicine, Beijing 100850, China. Tel.: +86 10 88215159; fax: +86 10 68214653.
E-mail address: jinyg@bmi.ac.cn (Y. Jin).

0378-5173/$ – see front matter © 2011 Elsevier B.V. All rights reserved.
doi:10.1016/j.ijpharm.2011.08.053

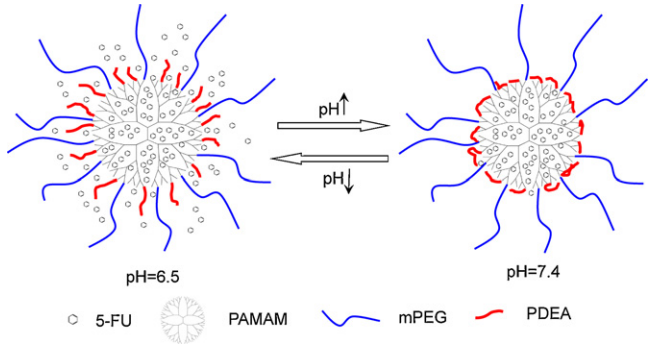

Fig. 1. Illustration of pH effect on the structure of PPD nanocarriers and their encapsulation and release of drugs. In the weakly acidic environments (pH 4.0 or 6.5) of buffered solutions and tumor tissues, the PDEA chains of PPD were hydrophilic and extended, so the drugs were free to enter or exit the nanostructure. In the neutral or weakly basic environments (pH 7.4 or 8.0) and in circulation, the PDEA chains of PPD were hydrophobic and contracted, so the drugs were tightly enclosed in the inner space.

dendrimer conjugates was stable, and the release of drug was slow (Patri et al., 2005). Stimulus-responsive dendrimers may address the above problem (Kojima, 2010). These stimulus factors include pH (Hui et al., 2005), temperature (Kono et al., 2007), and photosensitivity (Nishiyama et al., 2009).

Poly(2-(N,N-diethylamino)ethyl methacrylate) (PDEA) is a pH-sensitive polymer containing tertiary amine groups. PDEA is hydrophobic in neutral or basic medium, but hydrophilic in acidic medium. Taking advantage of this property, some pH-responsive copolymers or nanoparticles were prepared through PDEA conjugation (Guo et al., 2009; Oishi and Nagasaki, 2010). Most tumor tissues have a lower pH environment (less than 7.0), so pH-responsive drug release is useful for anticancer treatment (Lee et al., 2008).

PDEA can be chemically attached to other polymers or nanoparticles to form pH-responsive copolymers or nanoparticles. The PDEA-attached carriers are then used to load anticancer agents or genes for cancer treatment for selective release in tumor tissues (Guo et al., 2009; Oishi and Nagasaki, 2010; Xu et al., 2006; Zhang et al., 2009).

A novel PAMAM derivative, poly(2-(N,N-diethylamino)ethyl methacrylate) with methoxy-poly(ethylene glycol)-poly(amido amine) (PPD) was synthesized in this study as a nanocarrier for 5-fluorouracil (5-FU), an anticancer agent, with high encapsulation efficiency, tumor targeting and rapid release in tumor tissues. In the acidic environment of a tumor, the hydrophilic PDEA chains facilitate rapid entry and release of drug molecules. In the neutral/basic medium of the blood, the hydrophobic PDEA chains trap drugs tightly within the PPD core (Fig. 1).

2. Materials and methods

2.1. Materials

5-FU was obtained from Shandong Boyuan Chemical Co. Ltd. (China). Methoxy-poly(ethylene glycol)$_{750}$ (mPEG$_{750}$) and 2-(N,N-diethylamino)ethyl methacrylate (DEA) were from Acros. Organic solvents were of analytical grade, and other chemicals were of reagent grade. A murine hepatoma H_{22} cancer cell line was a gift from Prof. Shoujun Yuan (Beijing Institute of Radiation Medicine, BIRM). Purified water was prepared with a Heal Force Super NW Water System (Shanghai Canrex Analytic Instrument Co. Ltd., China) and was always used unless otherwise indicated. Infrared (IR) spectrum and ^{1}H nuclear magnetic resonance (NMR) (400 MHz) spectrum were recorded on a Bio-Rad FTS-65A infrared ray spectrometer and a JNM-ECA-400 NMR spectrometer, respectively.

2.2. Animals

Female Kunming mice from the Laboratory Animal Center of BIRM were used. All animal handling and surgical procedures were strictly conducted according to the Guiding Principles for the Use of Laboratory Animals. This study was approved by the Animal Care Committee of the Beijing Institute of Radiation Medicine. Mice were sacrificed to obtain tissues. Mice tissue homogenates used in the tissue distribution experiment were prepared in tissue/water (1:1, w/w). All studies were conducted in accordance with the Declaration of Helsinki.

2.3. Synthesis of PPD

The synthesis of PPD consisted of three steps. First, 4.0 G PAMAM dendrimers were synthesized using a stepwise, divergent strategy reported in the literature (Boas et al., 2006; Tomalia et al., 1985). The second step involved the combination of mPEG and PAMAM to obtain mPEG–PAMAM. Finally, mPEG–PAMAM was coupled to PDEA using atom transfer radical polymerization (ATRP) to obtain mPEG–PAMAM–PDEA (i.e., PPD). The detailed synthetic process is described as follows, and the route is shown in Fig. 2.

The 4.0 G PAMAM was synthesized with ethylene diamine as the initial core using Michael alkylation with methyl acrylate to yield a tertiary amine as the branching point. This was followed by aminolysis of the methyl ester (Boas et al., 2006; Newkome et al., 2001; Tomalia et al., 1985, 1986). There were 64 terminal amine groups found on each 4.0 G PAMAM molecule. The structure of 4.0 G PAMAM was consistent with other reports (Tomalia et al., 1985). IR (KBr) ν_{max}: 3429.4, 3078.1, 2930.2, 2850.8, 1636.5, 1549.7, 1125.7, 1197.0, and 581.0 cm^{-1}. ^{1}H NMR (DMSO-d_6) δ_H: 7.62 (CONH), 3.23, 2.70, 2.29, 2.27, 2.24, 2.13, (the above δ_H attributed to the ethylene hydrogen), 1.82 (terminal NH_2) ppm.

The above PAMAM (2.8 g, 0.2 mmol) was dissolved in formic acid and then mixed with mPEG750 (0.0225 g, 0.03 mmol). Excess formaldehyde was added to the above solution and the reaction was stirred for 24 h. The solution was then filtered, and the filtrate was placed in a dialysis bag (cut MW, 7000 Da, Union Carbide Co., USA) against water for 48 h, refreshing the water every 4 h. The solution in the bag was distilled under vacuum to remove most of the water, and the resulting product was then freeze-dried to obtain a gel of mPEG–PAMAM. IR (KBr) ν_{max}: 3433.6, 2920.7, 2148.7, 1634.1, 1558.7, 1463.7, 1350.7, 1293.4, 1249.9, 1101.3, 949.0, and 586.4 cm^{-1}.

The above mPEG–PAMAM (2 g, 0.1 mmol) was dissolved in 0.1 M NaOH with stirring for 12 h to obtain a slightly white, viscous solution. Excess chloroacetyl chloride (3 ml or more) was slowly added dropwise into the solution followed by agitation at room temperature for 24 h. The solution was dialyzed against water for 72 h as above, distilled under vacuum to remove water, and then freeze-dried to obtain a gel of mPEG–PAMAM–Cl that was stored under vacuum.

The mPEG–PAMAM–Cl gel (2.2 g, 0.1 mmol) was dissolved in methanol/water (1:1, v/v, 20 ml) under nitrogen. DEA (1.9 g, 1 mmol), cuprous bromide (CuBr, 0.144 g, 0.1 mmol), and bipyridine (bpy, 0.313 g, 0.2 mmol) were then added, and the resulting mixture was stirred at 50 °C for 12 h. A blue suspension was obtained and was subjected to dialysis against water for 72 h as above. The suspension was then distilled under vacuum to produce a light blue, viscous solid that was purified on an Al_2O_3 chromatographic column using methanol as the elution solvent. The recovered solution was distilled to obtain PPD as a white powder. IR (KBr) ν_{max}:

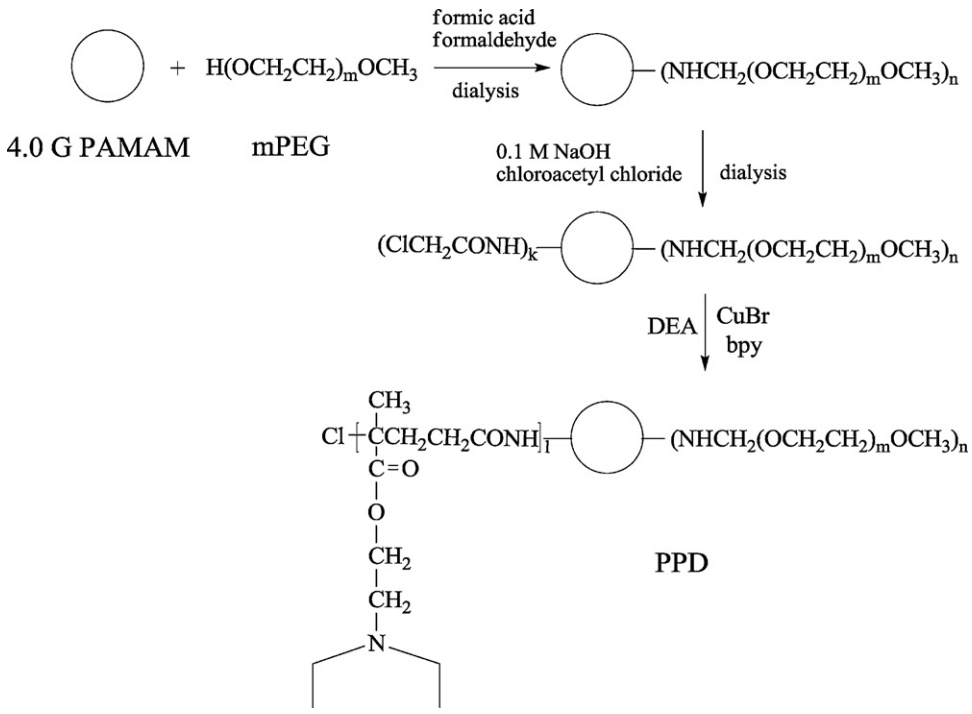

Fig. 2. The synthetic routes for poly(2-(N,N-diethylamino)ethyl methacrylate)-co-methoxy-poly(ethylene glycol)-poly(amidoamine) (PPD). (a) Formic acid; (b) formaldehyde; (c) dialysis; (d) 0.1 M NaOH; (e) chloroacetyl chloride and (f) dialysis.

3415.7, 3091.5, 2850.3, 1626.2, 1361.5, 1399.2, 1090.2, 1019.2, and 702.1 cm^{-1}.

2.4. HPLC determination of 5-FU

High-performance liquid chromatographic (HPLC) experiments were performed on a Shimadzu 10Avp HPLC system (Japan) consisting of a LC-10Avp pump, an SPD-10Avp UV detector, an SCL-10Avp controller, and Shimadzu CLASS-VP 6.12 chromatographic workstation software. The Diamonsil C18-ODS HPLC column (5 μm, 250 mm × 4.6 mm) and the EasyGuard C18-ODS HPLC guard column (5 μm, 8 mm × 4 mm) were purchased from Dikma Co. Ltd. (China). A manual injection valve and a 20-μl loop (7725i, Rheodyne, USA) were used. The UV detector was set at 266 nm, and the HPLC column temperature was maintained at 30 °C with an AT-950 heater and cooler (Tianjin Automatic Science Instrument Co. Ltd). The mobile phase for 5-FU measurement was methanol/water (10/90, v/v) with a flow rate of 0.8 ml/min. The retention time (t_R) of 5-FU was 6.1 min under these conditions. 5-FU in aqueous solution and PPD suspensions were diluted with the mobile phase before analysis. For the plasma and tissue homogenate samples, 10 μl was mixed with 0.1 M HCl (20 μl) and 70 μl of saturated $(NH_4)_2SO_4$ solution, followed by vortexing. The samples were then centrifuged at 5000 × *g* for 10 min and the supernatant was measured as above.

2.5. Preparation of 5-FU-loaded PPD nanocarriers

5-FU and PPD were dissolved in a buffered solution (Buffer I, pH 4.0) followed by adjustment to pH 8.0 with 0.1 M NaOH. The 5-FU-loaded PPD nanocarrier was then separated on a Sephadex G75 gel column with water or the buffered solution (Buffer II) at 4.0 ml/min. The encapsulation efficiency and loading content of drug were calculated. Buffer I was chosen with a pH of 4.0 (50 mM phosphate buffered solution, PBS) because PPD was insoluble in basic media. The optimal preparation method was determined based on the encapsulation efficiency of the drug.

2.6. Characterization of PPD nanocarriers

The PPD nanocarrier was observed using a Philips CM120 80-kV transmission electron microscope (TEM). The suspension (5 μl) containing PPD was dropped onto carbon-coated copper nets and set for 1 min; then the bulk of the solution was removed by filter paper from the edge of the nets. A solution containing 2% sodium phosphotungstate (pH 6.5) was also dropped onto the above spread nets, and processed as above. The obtained negative-stained samples were air-dried at room temperature and moved to TEM for observation as soon as possible. The dynamic lighting scattering (DLS) method on a Zetasizer Nano ZS (Malvern, UK) was used to measure the sizes of the PPD nanocarrier at different pH values. The zeta potentials of PPD nanocarriers were also measured with the above instrument at the room temperature.

2.7. Release of 5-FU from PPD nanocarriers

The release of 5-FU from PPD nanocarriers was measured using a dialysis method. A 5-FU-loaded PPD suspension (2 ml, 2 mg/ml 5-FU) was sealed in a dialysis bag (cut MW, 3500 Da) and dialyzed against PBS (145 ml, 50 mM, pH 6.5 or 7.4) in an oscillating incubator (100 rpm, 37 °C). Aliquots of the buffered solution (5 ml) were removed at predetermined time points between 0 and 10 h, supplementing the dialysis with the same amount of media (5 ml). The released 5-FU was determined using HPLC, and the cumulative release was calculated. The release of a free 5-FU solution in PBS was also measured as the control.

2.8. Tumor implantation

H_{22} cancer cells were extracted from the abdominal dropsy of mice bearing cancer cells and diluted with 0.9% NaCl to achieve a cell concentration of 2×10^7/ml. A 0.2 ml aliquot of cell suspension was subcutaneously injected into mice (16–20 g) under the right forelimb. One day after the transplant, the injected mice were selected for the next pharmacodynamic study. In addition, tumors

were allowed to develop for 7 days to reach about 1000 mm^3 in volume, and mice weighing 16–20 g were ready for pharmacokinetic and tissue distribution studies.

2.9. In vivo behavior of 5-FU-loaded PPD nanocarriers

The 5-FU-loaded nanocarriers were prepared as above, containing 3 mg/ml 5-FU, and sterilized by passing through 0.22 μm filters in advance. The administered dose was 25 mg/kg with a bolus i.v. injection via the mouse tail vein. The animals used included healthy mice and mice bearing H_{22} cancer cells. Approximately 100 μl of blood was collected from the tails and put into heparinized centrifuge tubes at 0, 2, 5, 10, 15, 20, 30, 60, 120, 240, 360, and 480 min. Plasma was separated using centrifugation at $1000 \times g$ for 5 min, and then 5-FU was determined using the above HPLC method. In the tissue distribution experiments, mice were administered nanocarriers i.v. and were sacrificed after 0.5, 1, 4, and 8 h. The tissues were then removed, weighed and disrupted to homogenates with water of equal volume following the same procedure used for plasma samples. Pharmacokinetic parameters were calculated with the 3p87 pharmacokinetic software supplied by Prof. H. Song of BIRM.

2.10. Pharmacodynamic study of 5-FU-loaded PPD nanocarriers

Mice with the expected tumor volume were divided into four groups with 5 mice in each group. The mice of Group I were i.v. injected via the tail vein with 0.9% NaCl solution as the blank control, and the mice of Group II were injected with 5-FU solutions in PBS (50 mM, pH 7.4, 25 mg 5-FU/kg dose) as positive control. The mice of Group III were injected with 5-FU-loaded PPD nanocarriers (3 mg/ml 5-FU, 25 mg 5-FU/kg dose) as the experimental group, and the mice of Group IV were injected with blank PPD suspensions alone (12.5 mg PPD/kg dose) as the carrier control.

Xenograft sizes were measured in two perpendicular dimensions using a caliper once a day after treatment. The first administration day was recorded as 0 day. Tumor volume (V) was calculated with the formula, $V = 0.5L \times W^2$, where L is the largest superficial diameter and W is the smallest superficial diameter of the xenograft. After seven days, the mice were sacrificed to weigh the tumors. Tumors were dissected and weighed to calculate the tumor inhibitory rate based on the following equation:

$$\text{Tumor inhibitory rate}\,(\%) = \frac{W_{\text{blank}} - W_{\text{test}}}{W_{\text{blank}}} \times 100$$

where W_{blank} and W_{test} were the tumor average weight of the control group and the test groups, respectively. Mice were weighed daily.

Statistically significant differences for multiple groups were determined using a one-way ANOVA with a Dunnett T3 test. All tests were performed using SPSS 16.0 software (SPSS Inc.).

3. Results and discussion

3.1. Encapsulation of 5-FU in PPD nanocarriers based on pH change

The PDEA chains of PPD changed from a charged hydrophilic state to a non-charged hydrophobic state with a pH change due to the pH-responsive tertiary amines. To entrap the drugs, a weakly acidic solution was used to dissolve 5-FU and PPD. After 5-FU diffused into the inner space of PPD, the medium was immediately adjusted to pH 8.0, making the PDEA chains hydrophobic and encasing the drugs. This procedure is illustrated in Fig. 1.

When Buffers I and II were pH 7.4 PBS, the encapsulation efficiencies were 42.1%, 62.5%, and 43.0% for the 1:1, 2:1, and 3:1 (wt/wt) ratios of 5-FU/PPD, respectively. Therefore, the 2:1 ratio was selected in the subsequent experiments. When Buffers I and II were pH 4.0 PBS, the encapsulation efficiency was 73.2%. Therefore, more space was provided to entrap drugs in the acidic media than in neutral media because the PDEA chains extended into the media under acidic conditions. When Buffer I was pH 4.0 PBS and Buffer II was pH 8.0 PBS, the encapsulation efficiency was as high as 92.5%. Therefore, an acid–alkaline transition process was the optimal preparation method for 5-FU-loaded PPD nanocarriers.

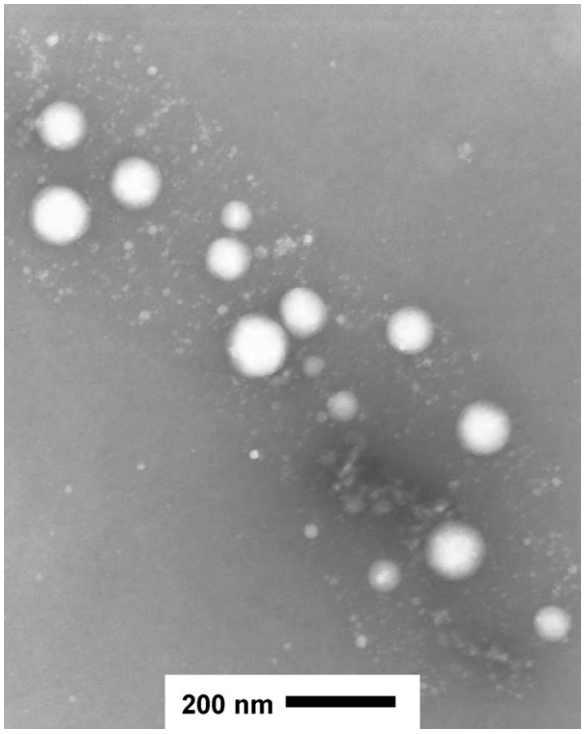

Fig. 3. The TEM images of the PPD nanocarriers.

3.2. Characteristics of the PPD nanocarrier at different pH

The PPD nanocarrier was spherical according to the TEM images (Fig. 3), in accordance with the theoretical model of PPD (Fig. 1). Interestingly, the dynamic sizes of PPD nanocarriers depended on pH. Specifically, the diameter of PPD was 43.0 nm at pH 4.0, 41.6 nm at pH 6.5, and 11.6 nm at 7.4. The pH dependency of the particle size was consistent with the above drug encapsulation procedure. Therefore, the expansion and contraction of PDEA chains at different pH values had a great influence on the size of the PPD nanocarriers (Fig. 1). The zeta potentials of PPD nanocarriers were different in the different pH media, which were 12.4, 9.7 and 7.1 mV at pH 4.0, 6.5 and 7.4, respectively. The positive potential is related to the existence of tertiary amines in the PDEA chains of PPD and the low pH media should improve the protonation of amines. The phenomena were also reported by the others (Karanikolopoulos et al., 2010; Oishi and Nagasaki, 2010).

3.3. pH-depended release of 5-FU from PPD nanocarriers

The release of 5-FU from PPD nanocarriers was highly pH-dependent. In comparison, free 5-FU released rapidly from the dialysis bag independent of pH. The release of entrapped 5-FU from PPD nanocarriers was slow at pH 7.4 (Fig. 4a), but the release of entrapped 5-FU at pH 6.5 was almost equal to that of free 5-FU (Fig. 4b). Furthermore, the release at pH 6.5 was almost 100% within 6 h, which was much faster than that at pH 7.4.

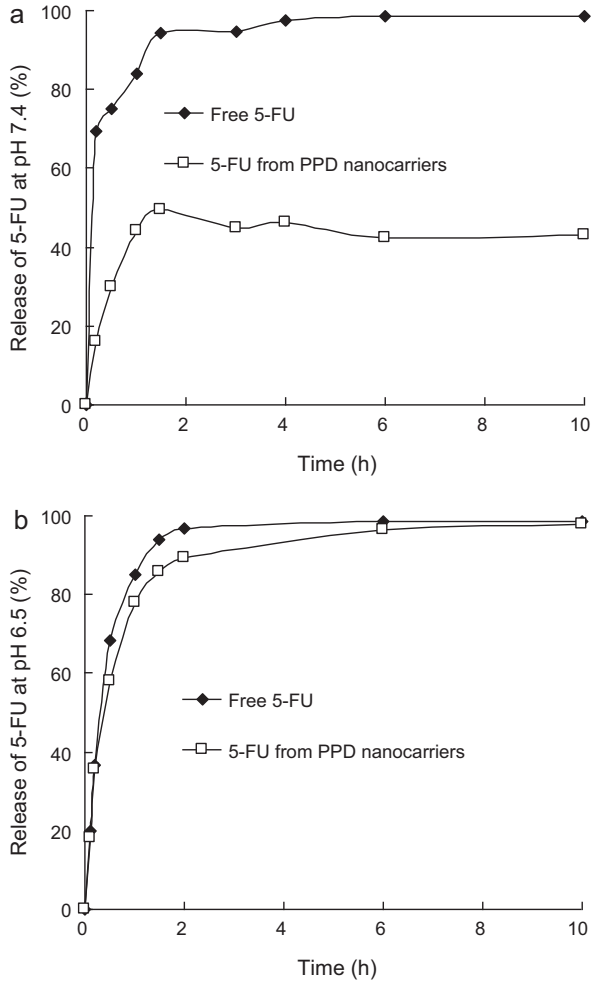

Fig. 4. The release of 5-FU at pH (a) 7.4 and (b) 6.5.

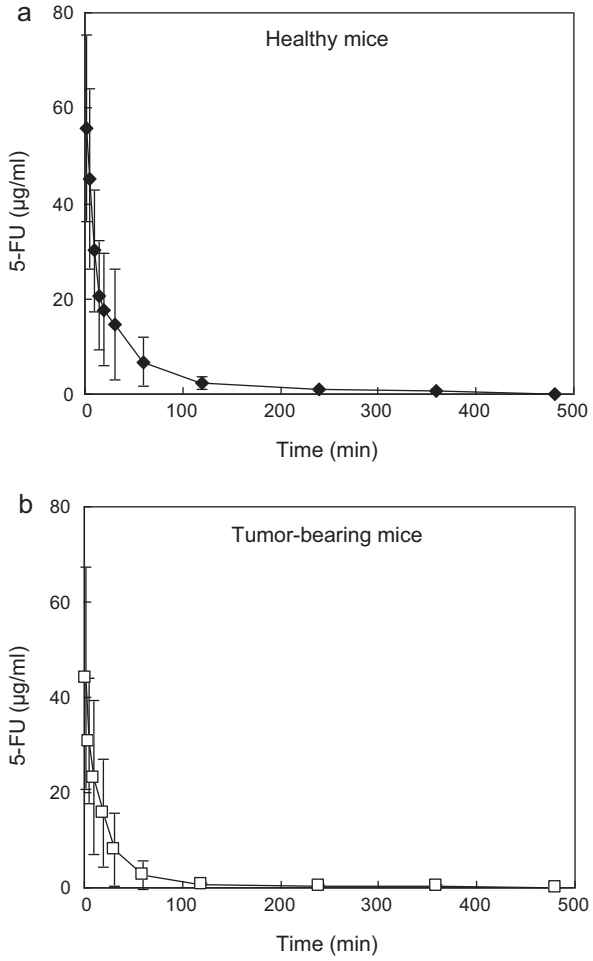

Fig. 5. Time course of 5-FU in (a) healthy mice and (b) tumor-bearing mice after i.v. administration of 5-FU-loaded PPD nanocarriers. The data represent the mean ± SD ($n = 5$).

The pH-depended release was consistent with the above drug encapsulation behavior of the PPD nanocarriers. The PDEA chains changed from their hydrophobic state at pH 7.4 to their hydrophilic state at pH 6.5, so the inner space of the PPD was open to release the entrapped drugs at lower pH (Fig. 1). Because tumors generally have a low pH, the pH-responsive release of 5-FU from PPD nanocarriers is favorable for cancer therapy.

3.4. Tumor targeting effect of 5-FU-loaded PPD nanocarriers

5-FU was rapidly distributed in the circulation after i.v. administration of 5-FU-loaded PPD nanocarriers to healthy or tumor-bearing mice (Fig. 5). A pharmacokinetic model of two chambers was thus expressed. The distribution half-lives ($t_{1/2\alpha}$) were 9.6 min in healthy mice and 9.5 min in tumor-bearing mice, and the elimination half-lives ($t_{1/2\beta}$) were 100 min in healthy mice and 72 min in tumor-bearing mice (Table 1). Generally, the mononuclear phagocyte system is the major distribution site of nanoparticulates, although long-circulating nanoparticles tend to distribute into tumor tissues due to the EPR effect (Moghimi et al., 2001). In fact, the comparison study between PEGylated PAMAM nanocarriers and non-PEGylated PAMAM nanocarriers was well performed by the other researchers with 5-FU as the model drug (Bhadra et al., 2003). They compared physicochemical parameters, hemolytic toxicity, drug entrapment, drug release and blood-level studies of both PEGylated and non-PEGylated systems. They found that the PEGylated nanocarriers increased their drug-loading capacity, reduced their drug release rate and hemolytic toxicity, and showed high stability at room temperature. More importantly, the PEGylated systems were suitable for the prolonged *in vivo* delivery of an anti-cancer drug. The long PEG chains would lead to PPD nanocarriers displaying long circulation times and having the opportunity to target tumors. In addition, the shorter $t_{1/2\beta}$ in tumor-bearing mice compared with the healthy mice could indicate rapid tumor distribution of 5-FU loaded in the nanocarriers.

Tissue distribution further showed the tumor-targeting effect of PPD nanocarriers. In healthy mice, the concentration of 5-FU was comparable in the liver, spleen, lungs, kidney and heart, although the concentration in blood was the highest within 1 h (Fig. 6a). Naked nanoparticulate systems were different, as they mainly distributed in the phagocyte-abundant liver, spleen and lungs (Ishida et al., 2002; Jin et al., 2006, 2009). Therefore, the PPD nanocarriers

Table 1
Pharmacokinetic parameters of 5-FU after i.v. administration of 5-FU-loaded PPD nanocarriers to mice with the dose of 25 mg 5-FU/kg.

Parameter	Healthy mice	Tumor-bearing mice
$V_{(C)}$ (ml)	10.31	18.18
$t_{1/2\alpha}$ (min)	9.62	9.50
$t_{1/2\beta}$ (min)	100.9	72.5
k_α (min^{-1})	0.09	0.08
k_β (min^{-1})	0.01	0.01
$AUC_{0-480\ min}$ ($\mu g\ ml^{-1}\ min$)	1573.2	840.8
Cl (ml/min^{-1})	0.48	1.02

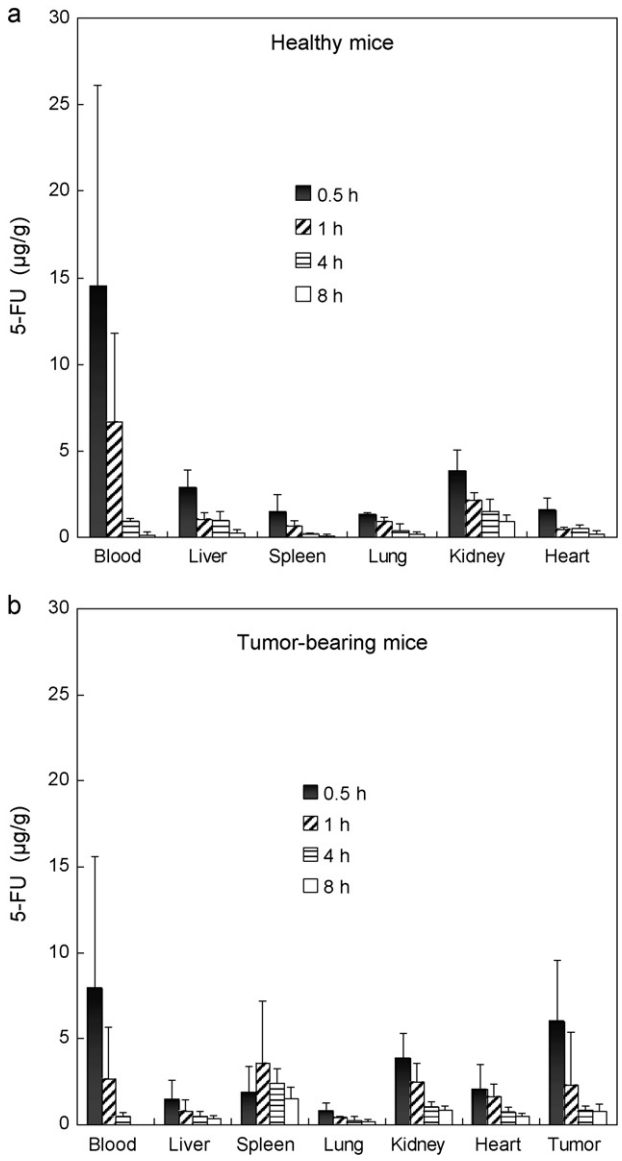

Fig. 6. Biodistribution of 5-FU in (a) healthy mice and (b) tumor-bearing mice after i.v. administration of 5-FU-loaded PPD nanocarriers. The data represent the mean ± SD ($n = 5$).

were considered to be long-circulating based on their pharmacokinetics and biodistribution (Lim et al., 2008; Moghimi et al., 2001).

The biodistribution of 5-FU in tumor-bearing mice was significantly different from that in healthy mice. The amounts of 5-FU in the blood, liver, spleen and lungs of tumor-bearing mice were less than that in healthy mice, whereas the amounts in the kidney and heart were similar (Fig. 6b). In contrast, drug accumulation in tumors was high. Interestingly, the concentration of 5-FU in tumors was much higher than that in the liver. Specifically, the concentration of 5-FU was as high as 6.01 μg/g in tumors at 0.5 h, 4 times that in the liver (1.45 μg/g). Therefore, it was concluded that high tumor targeting was achieved with the PPD nanocarriers. Additionally, based on the above-described pH-responsive release of 5-FU from PPD nanocarriers, the rapid release of 5-FU into tumors could also improve the accumulation of drugs in tumor tissue.

3.5. Enhanced anticancer effect of 5-FU-loaded PPD nanocarriers

Tumor volume was determined from the third day because the tumors were small in the first two days. However, from the fourth

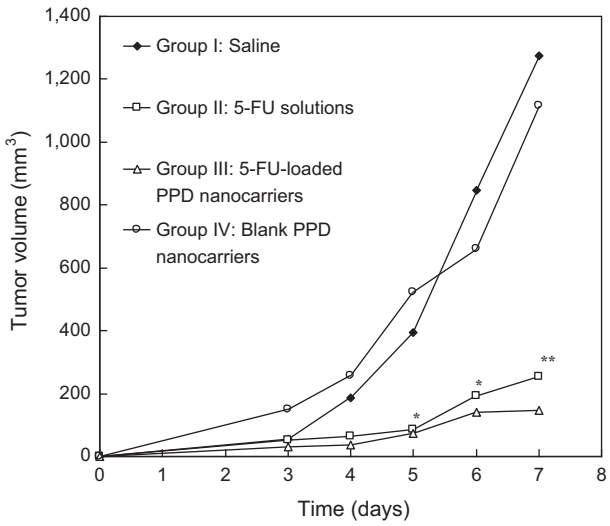

Fig. 7. Tumor volume profile of mice. *$p < 0.05$, Group III vs. Group I; **$p < 0.01$, Group III vs. Group IV.

day, a significant difference between the volumes of Group III (5-FU-loaded PPD nanocarriers) and Group I (saline, blank control) tumors was discovered (Fig. 7). After 7 days administration, Group III had much smaller tumors than Group II (5-FU solutions). Finally, the tumor volumes of Groups I, II, III and IV were 1274, 253, 148, and 1115 mm^3, respectively, and the differences are clearly shown in the tumor graphs (Fig. 8). The mean tumor weights of Groups I, II, III and IV were 1.16 ± 0.20 g, 0.20 ± 0.03 g, 0.08 ± 0.01 g, and 1.12 ± 0.17 g (mean ± SD, $n = 5$), respectively. Significant differences were shown between any two groups ($p < 0.01$) except Group I and Group IV. The tumor inhibitory rates of Group II and III were 82.9% and 93.2%, respectively. Interestingly, the body weight of all experimental mice increased by 50.3%, 23.1%, 17.3%, and 49.0% for Groups I, II, III and IV, respectively. In addition, the saline control group and the PPD carrier group had similar tumor volumes during the entire experiment. Therefore, PPD alone had no toxicity. The smaller body weight increases of Groups II and III were due to the growth of small tumors, whereas the largest body weight increases of Group I and IV resulted from the rapid growth of tumors. The better anticancer activity of Group III than Group II demonstrated the enhanced anticancer effect using 5-FU-loaded PPD nanocarriers. Tumor specific targeting and pH-responsive rapid drug release were the major reasons for this enhancement in efficacy.

3.6. Future design of pH-responsive dendrimer nanocarriers

pH-responsive drug release is a useful strategy for anticancer drug delivery. But it is not enough. In addition to pH-response, many other important factors need to be considered when designing an ideal tumor-targeted drug delivery system. The most

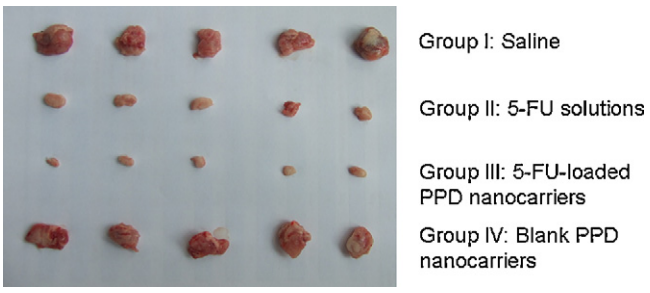

Fig. 8. Photographs of the mouse tumors.

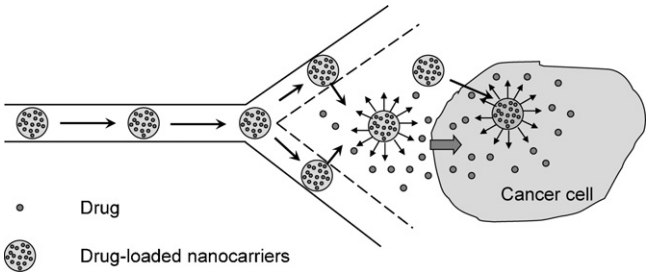

Fig. 9. Illustration of the *in vivo* process of ideal anticancer agent nanocarriers.

important point is to maintain an effective dose of a drug within tumors. Three factors are necessary to achieve this goal: (a) high encapsulation of drugs in the delivery systems, (b) high tumor specific targeting, and (c) sufficient drug accumulation or controlled release in tumors.

The entire circulation and drug release process of an optimal anticancer agent carrier is illustrated in Fig. 9. Tumor targeting is determined by the size, charge, shell, and surface functional groups of the carriers. However, high drug encapsulation can be difficult to achieve, and drug leakage can occur during storage or circulation.

The design of PPD nanocarriers is based on the need to solve these problems of anticancer drugs. PAMAM is a well-defined nanostructure with a large inner space that is capable of entrapping a number of small molecules. The attached mPEG chains prolong the circulation time of carriers and lead to tumor targeting. PDEA is pH-responsive with a specific pH turning point that enables high drug encapsulation and rapid release in tumors. The above functions were combined in the PPD nanocarriers investigated in this study. Fortunately, high drug encapsulation, slow leakage, high stability, long circulation time, tumor targeting, and pH-responsive release were all achieved using these PPD nanocarriers.

Some questions still remained in spite of the excellent performance of the well-designed PPD nanocarriers. 5-FU-loaded PPD nanocarriers did not show significantly better anticancer effects than free 5-FU. The initial administration time might therefore affect treatment. The administration began from the second day of tumor transplant when the tumors were not well established. Another possible reason for treatment not well might have been the manner of attachment of the pH-responsive groups and the PEG chains. Specifically, the attachment of mPEG and PDEA chains was parallel, so when the PDEA chains shortened upon pH transition, the inner space might have incompletely sealed because the adjacent mPEG chains hindered shrinking. Therefore, we will improve our design of functional PAMAM derivatives in the future (e.g., by attaching mPEG and PDEA chains to the PAMAM surface in a different configuration to avoid interruption).

4. Conclusion

A novel, long-circulating and pH-responsive PPD nanocarrier based on a PAMAM dendrimer was prepared in this study. It was found to be promising as a carrier of anticancer agents because of its high drug encapsulation, high tumor targeting and rapid release of drugs in low-pH tumor tissues. The drug-loaded carrier could therefore be an exciting anticancer nanomedicine.

Acknowledgements

This work was supported by the National Key Technologies R&D Program for New Drugs (No. 2009ZX09301-002) and the National Natural Science Foundation of China (No. 30772672). We thank Prof. S. Yuan for supplying the cancer cell line.

References

Amiji, M.M., 2007. Nanotechnology for Cancer Therapy. Taylor & Francis, CRC Press, Boca Raton, FL.
Bhadra, D., Bhadra, S., Jain, S., Jain, N.K., 2003. A PEGylated dendritic nanoparticulate carrier of fluorouracil. Int. J. Pharm. 257, 111–124.
Boas, U., Christensen, J.B., Heegaard, P.M.H., 2006. Dendrimers: design, synthesis and chemical properties. J. Mater. Chem. 16, 3785–3798.
Boas, U., Heegaard, P.M.H., 2004. Dendrimers in drug research. Chem. Soc. Rev. 33, 43–63.
Cho, K., Wang, X., Nie, S., Chen, Z.G., Shin, D.M., 2008. Therapeutic nanoparticles for drug delivery in cancer. Clin. Cancer Res. 14, 1310–1316.
Esfand, R., Tomalia, D.A., 2001. Poly(amidoamine) (PAMAM) dendrimers: from biomimicry to drug delivery and biomedical applications. Drug Discov. Today 6, 427–436.
Gillies, E.R., Fréchet, J.M.J., 2005. Dendrimers and dendritic polymers in drug delivery. Drug Discov. Today 10, 35–43.
Guo, R., Li, R., Li, X., Zhang, L., Jiang, X., Liu, B., 2009. Dual-functional alginic acid hybrid nanospheres for cell imaging and drug delivery. Small 5, 709–717.
Hui, H., Xiao-dong, F., Zhong-lin, C., 2005. Thermo- and pH-sensitive dendrimer derivatives with a shell of poly (N,N-dimethylaminoethyl methacrylate) and study of their controlled drug release behavior. Polymer 46, 9514–9522.
Ishida, T., Harashima, H., Kiwada, H., 2002. Liposome clearance. Biosci. Rep. 22, 197–224.
Iyer, A.K., Khaled, G., Fang, J., Maeda, H., 2006. Exploiting the enhanced permeability and retention effect for tumor targeting. Drug Discov. Today 11, 812–818.
Jin, Y., Ai, P., Xin, R., Tian, Y., Dong, J., Chen, D., Wang, W., 2009. Self-assembled drug delivery systems. Part 3. In vitro/in vivo studies of the self-assembled nanoparticulates of cholesteryl acyl didanosine. Int. J. Pharm. 368, 207–214.
Jin, Y.G., Tong, L., Ai, P., Li, M., Hou, X.P., 2006. Self-assembled drug delivery systems. 1. Properties and in vitro/in vivo behavior of acyclovir self-assembled nanoparticles (SAN). Int. J. Pharm. 309, 199–207.
Karanikolopoulos, N., Zamurovic, M., Pitsikalis, M., Hadjichristidis, N., 2010. Poly(DL-lactide)-b-poly(N,N-dimethylamino-2-ethyl methacrylate): synthesis, characterization, micellization behavior in aqueous solutions, and encapsulation of the hydrophobic drug dipyridamole. Biomacromolecules 11, 430–438.
Kojima, C., 2010. Design of stimuli-responsive dendrimers. Expert Opin. Drug Deliv. 7, 307–319.
Kojima, C., Kono, K., Maruyama, K., Takagishi, T., 2000. Synthesis of polyamidoamine dendrimers having poly(ethylene glycol) grafts and their ability to encapsulate anticancer drugs. Bioconjugate Chem. 11, 910–917.
Kono, K., Miyoshi, T., Haba, Y., Murakami, E., Kojima, C., Harada, A., 2007. Temperature sensitivity control of alkylamide-terminated poly(amidoamine) dendrimers induced by guest molecule binding. J. Am. Chem. Soc. 129, 7222–7223.
Lee, E.S., Gao, Z., Bae, Y.H., 2008. Recent progress in tumor pH targeting nanotechnology. J. Control. Release 132, 164–170.
Lim, J., Guo, Y., Rostollan, C.L., Stanfield, J., Hsieh, J.-T., Sun, X., Simanek, E.E., 2008. The role of the size and number of polyethylene glycol chains in the biodistribution and tumor localization of triazine dendrimers. Mol. Pharm. 5, 540–547.
Moghimi, S.M., Hunter, A.C., Murray, J.C., 2001. Long-circulating and target-specific nanoparticles: theory to practice. Pharmacol. Rev. 53, 283–318.
Newkome, G.R., Moorefield, C.N., Vogtle, F., 2001. Dendrimers and Dendrons: Concepts, Syntheses, Applications. Wiley-VCH Verlag GmbH & Co., Plankstadt.
Nishiyama, N., Morimoto, Y., Jang, W.D., Kataoka, K., 2009. Design and development of dendrimer photosensitizer-incorporated polymeric micelles for enhanced photodynamic therapy. Adv. Drug Deliv. Rev. 61, 327–338.
Oishi, M., Nagasaki, Y., 2010. Stimuli-responsive smart nanogels for cancer diagnostics and therapy. Nanomedicine 5, 451–468.
Patri, A., Kukowska-Latallo, J., Baker, J., 2005. Targeted drug delivery with dendrimers: comparison of the release kinetics of covalently conjugated drug and non-covalent drug inclusion complex. Adv. Drug Deliv. Rev. 57, 2203–2214.
Svenson, S., Tomalia, D.A., 2005. Dendrimers in biomedical applications – reflections on the field. Adv. Drug Deliv. Rev. 57, 2106–2129.
Tomalia, D.A., Baker, H., Dewald, J., Hall, M., Kallos, G., Martin, S., Roeck, J., Ryder, J., Smith, P., 1985. A new class of polymers: starburst-dendritic macromolecules. Polym. J. 17, 117–132.
Tomalia, D.A., Baker, H.J.D., Hall, M., Kallos, G., Martin, S., Raeck, J., Ryder, J., Smith, P., 1986. Dendritic macromolecules: synthesis of starburst dendrimers. Macromolecules 19, 2466–2468.
Xu, P., Kirk, E.A.V., Murdoch, W.J., Zhan, Y., Isaak, D.D., Radosz, M., Shen, Y., 2006. Anticancer efficacies of cisplatin-releasing pH-responsive nanoparticles. Biomacromolecules 7, 829–835.
Zhang, B., Kanapathipillai, M., Bisso, P., Mallapragada, S., 2009. Novel pentablock copolymers for selective gene delivery to cancer cells. Pharm. Res. 26, 700–713.